A method to analyze current mismatch in a multijunction laser power converter based on I–V measurements

An-Cheng Wang,[1,2] (iD) Yu-Run Sun,[1,2,a] Shu-Zhen Yu,[2] Jia-Jing Yin,[1,2] (iD) Wei Zhang,[2] Jun-sheng Wang,[2] Qiu-Xue Fu,[1,2] and Jian-Rong Dong[1,2,a]

AFFILIATIONS

[1]School of Nano-Tech and Nano-Bionics, University of Science and Technology of China, Hefei 230026, China
[2]Key Laboratory of Nano Devices and Applications, Suzhou Institute of Nano-Tech and Nano-Bionics,
 Chinese Academy of Sciences, Suzhou 215123, China

[a]Authors to whom correspondence should be addressed: yrsun2011@sinano.ac.cn and jrdong2007@sinano.ac.cn

ABSTRACT

Multiple steps are observed in the I–V curves of current-mismatched six-junction InGaAs laser power converters with the voltage ranging from reverse breakdown voltage to open circuit voltage. The formation mechanism of the I–V curves is analyzed using a series-connected device model. The voltage drops across subcells can be significantly different at a certain current, and the steps represent the subcell photocurrents. The photocurrents of subcells are experimentally determined, and the degree of current mismatch is obtained for a multijunction laser power converter (MJLPC), which provides useful information for the design and fabrication of high-efficiency MJLPC. In addition, the absorption coefficient of InGaAs is extracted based on the current mismatch degrees at different temperatures, providing another way to determine the active layer absorption coefficient of an MJLPC.

Published under an exclusive license by AIP Publishing. https://doi.org/10.1063/5.0048466

The multijunction laser power converter (MJLPC) is an efficient energy-conversion device and has attracted increasing attention due to its advantages in terms of high output voltage and anti-electromagnetic interference.[1–9] ∼1500 nm lasers have been widely used in communication[10] and medical domains[11] because of their low transmission loss in fibers[12] and their ability to easily penetrate the skin. InGaAs MJLPC is a potential candidate to power medical implants in the human body with a ∼1500 nm laser as the power source, this would relieve patients of the burden of having to undergo multiple surgeries throughout their lives to change batteries.[13] The current of a multijunction photovoltaic converter is limited by the subcell producing the minimum photocurrent, and the optimal performance can be obtained only when all subcells generate the same current, i.e., current matched.[14] Therefore, the most important issue in terms of fabricating a high-efficiency MJLPC is to design a current-matched MJLPC epitaxial structure, which depends on the absorption coefficient of the active layers. However, published absorption coefficients of InGaAs at ∼1500 nm exhibit non-trivial variability,[15–17] which poses difficulties in terms of designing current-matched MJLPCs. External quantum efficiency (EQE) measurements[18,19] are often used to assess the performance of

subcells of a multijunction solar cell and to obtain information regarding the subcell currents as well as the current mismatch among subcells assisted by the standard solar spectrum, thereby providing feedback for device design. However, EQE measurement is not an effective approach for evaluating the current mismatch in an MJLPC, since none of the subcells of the same material can be selectively measured by biasing other subcells with monochromatic lights, as in the case of multiple junction solar cells where subcells absorb different segments of the solar spectrum. So far, no method has been put forward to characterize the current mismatch degree in an MJLPC, which makes it difficult and time-consuming to optimize MJLPC efficiency.

In this Letter, I–V measurements of a six-junction InGaAs LPC under 1520 nm laser illumination are undertaken from reverse breakdown voltage to open circuit voltage. Steps are observed and analyzed based on the series-connected device model. It is found that the steps reflect the subcell photocurrents. Therefore, the subcell photocurrents as well as the current mismatch of the six-junction InGaAs LPC are obtained from the I–V curves. The absorption coefficient of InGaAs is also extracted by a combination of calculation and temperature-dependent I–V measurements of the InGaAs MJLPCs.

The epitaxial structure of the six-junction InGaAs LPC under investigation was designed and grown by a metal-organic chemical vapor deposition (MOCVD) system. The thicknesses of subcells adopted in the design of the six-junction InGaAs LPC are shown in Table I. The I–V characteristics of the LPCs illuminated by a 1520 nm laser were measured using the four-wire method to eliminate the effects of series resistance introduced by wires. To minimize the temperature increase during I–V measurements, LPC chips were placed on copper-plated ceramic heat sinks with silver paste in between and each I–V curve was obtained within 2 s laser illumination. Temperature-dependent I–V measurements in the range of 300–453 K were taken under a constant laser power with the MJLPC placed on a temperature-controlled plate.

To investigate MJLPCs, attention is usually paid to the I–V characteristics under forward bias, and the parameters of the device are obtained, thereby,[1–9,20,21] but the segment of the I–V curve under reverse bias is often ignored. In our experiments, MJLPCs are characterized from reverse breakdown voltage to open circuit voltage, and the I–V curves of a six-junction InGaAs LPC under different 1520 nm laser powers are shown in Fig. 1(a). It can be seen that steps are observed in each curve except for the dark curve. This multi-step I–V curve has not, hitherto, been reported and provides very useful information concerning the current mismatch in the MJLPC as discussed later. To facilitate the discussion, the six-junction LPC is represented by six series-connected PN junctions, i.e., six subcells, as shown in Fig. 1(b). When the thicknesses of the MJLPC are not well designed, the photocurrents of subcells differ under laser illumination. As a result, the current of the MJLPC is constrained by the minimum one of the subcells attributed to the series connection of the subcells, and the photo-generated voltages across the subcells could be significantly different. The total voltage V across an MJLPC is the sum of all subcell voltages and given by

$$V = V_1 + V_2 + V_3 + V_4 + V_5 + V_6. \quad (1)$$

Therefore, the differential resistance of an MJLPC is expressed by

$$\frac{\partial V}{\partial I} = \frac{\partial (V_1 + V_2 + V_3 + V_4 + V_5 + V_6)}{\partial I} = \sum_{i=1}^{6} \frac{\partial V_i}{\partial I}. \quad (2)$$

To understand the I–V characteristics of the MJLPC, I–V curves of a reference single-junction InGaAs LPC with the same N- and P-type doping concentrations as the InGaAs MJLPC are measured under different 1520 nm laser powers [Fig. 2(a)]. As can be seen, the reverse breakdown voltage V_{BR} is almost independent of the laser power, and the current between V_{BR} and V_M (voltage at maximum

TABLE I. The thicknesses of subcells of the six-junction InGaAs LPC.

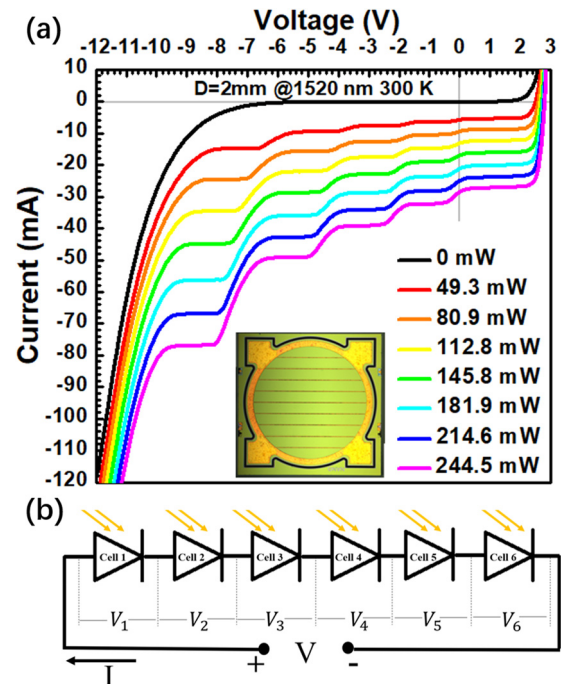| Subcell	Thickness (nm)
1	154
2	184
3	241
4	352
5	586
6	2306

FIG. 1. (a) Measured I–V characteristics of a six-junction InGaAs LPC under different laser powers. The inset shows an image of a cell with an aperture diameter of 2 mm. (b) Simplified schematic circuit model of the six-junction laser power converter. The positive current direction is represented by the arrows.

power point) is roughly a constant proportional to the illumination power. Figure 2(b) shows that the differential resistance of the LPC presents a spike of several thousand ohms as the current reaches its photocurrent and becomes small at other currents. Therefore, according to Eq. (2), once the current of the MJLPC reaches the photocurrent of one of the subcells, the differential resistance of the MJLPC is mainly determined by this subcell while those of other subcells with different photocurrents can be neglected,

$$\lim_{I \to I_{Li}} \frac{\partial V}{\partial I} \approx \lim_{I \to I_{Li}} M_i \frac{\partial V_i}{\partial I}, \quad i = 1, 2, 3 \ldots N, \quad (3)$$

where I_{Li} is the photocurrent of subcell i, M_i is the number of subcells generating I_{Li}, and N is the number of subcells in the MJLPC. It is implied by Eq. (3) that there will be N steps in the I–V curves of the N-junction LPC if subcell photocurrents are different from each other ($M_i = 1$, i = 1, 2, …N) and the width of each step is about V_M–V_{BR}. Otherwise, the number of steps will be reduced when M_i ($M_i \geq 2$) subcells generate the same photocurrent, and the width of the combined steps of the same height will be expanded to $M_i(V_M$–$V_{BR})$.

Figure 3 schematically shows the shaping of a measured I–V curve of the six-junction InGaAs LPC by the I–V curves of the six subcells. As the voltage changes from open circuit voltage to reverse breakdown voltage, the current will increase from zero. Once the current reaches the lowest photocurrent of the subcells, the MJLPC current will be clasped by the subcell due to its large differential resistance, which corresponds to the first step in the I–V curve, i.e., BC in Fig. 3(a). Furthermore, reducing the voltage pushes the subcell of
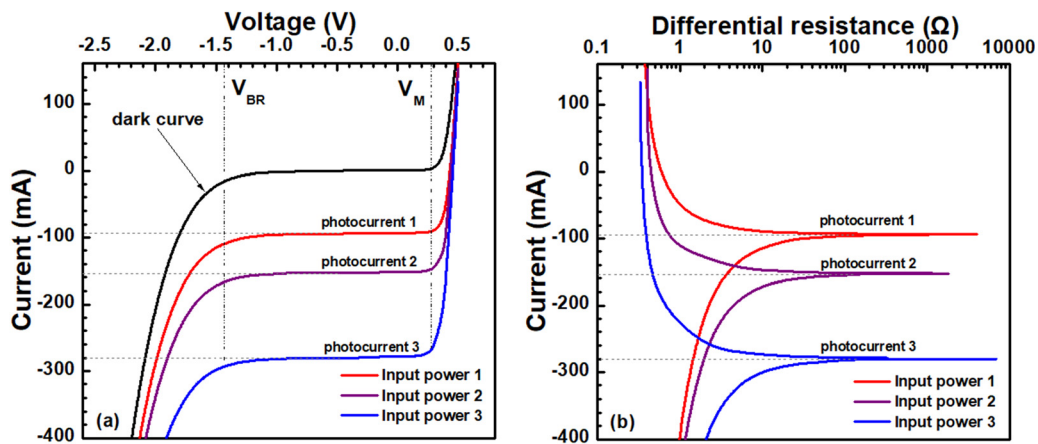
FIG. 2. (a) I–V curves of a reference single-junction InGaAs LPC. (b) Differential resistance as a function of current at various 1520 nm illumination powers.

the lowest photocurrent into the reverse breakdown state, i.e., CD, where the current increases with the voltage again until it reaches the second lowest photocurrent, and then, the current is clasped by this subcell leading to the step DE. The remaining subcells will undergo a similar process, in turn, as the voltage keeps reducing, which corresponds to the steps FG, HI, and JK. Finally, all subcells are reversely broken down and the current will increase significantly with the voltage. However, five instead of six steps are observed in Fig. 3(a) and the BC step is almost twice as wide as the other steps, which implies that the photocurrents of subcells a and b are quite close and indiscernible as shown in Fig. 3(b). The two steps of the same height are combined to form an extended step BC. Due to the large current mismatch of the MJLPC under illumination, even when the voltage of the MJLPC is 0 V, the relatively low photocurrent of subcells a and b restrains the current of the MJLPC. As a result, the voltages of the other four subcells are near the open circuit voltage, ∼0.5 V, subcells a and b are biased around

−1 V according to Eq. (1), and the MJLPC is at a state between point C and D as shown in Fig. 3(a).

In general, steps in the I–V curve of a current-mismatched MJLPC correspond to the respective photocurrents of subcells, and therefore, the subcell photocurrents can be obtained. Table II shows the photocurrents of the six subcells obtained from the I–V curves of an MJLPC under different 1520 nm laser powers as well as the current mismatch degree defined by

$$C_m = \left| \frac{\sqrt{\frac{1}{N} \sum_{i=1}^{N} \left(I_i - \overline{I}\right)^2}}{\overline{I}} \right|, \tag{4}$$

where I_i is the subcell photocurrent, $\overline{I}$ is the mean value of the subcell photocurrents, and N is the number of subcells. It is expected that C_m will decrease with increasing incident laser power because of luminescence coupling.[22–26] However, the data shown in Table II illustrate
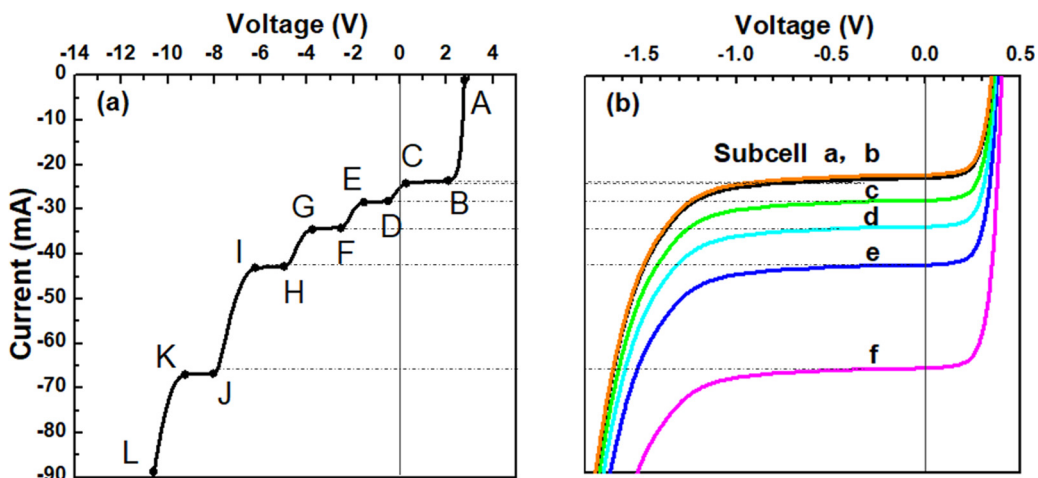

FIG. 3. (a) Schematics to show the shaping of the I–V characteristics of a six-junction LPC by superposition of (b) the I–V curves of the six subcells.

TABLE II. Extracted photocurrents for subcells of a six-junction InGaAs LPC.

Laser power (mW)	Photocurrent (mA)						C_m
	Subcell a	Subcell b	Subcell c	Subcell d	Subcell e	Subcell f	
49.3	−5.279	−5.279	−6.294	−7.648	−9.408	−14.687	0.44 337
80.9	−8.596	−8.799	−10.355	−12.521	−15.635	−24.433	0.44 937
112.8	−12.318	−−12.521	−14.687	−17.597	−21.861	−34.518	0.45 011
145.8	−16.041	−16.041	−19.154	−22.809	−28.494	−44.873	0.44 933
181.9	−19.898	−20.305	−23.824	−28.697	−36.074	−56.176	0.44 901
214.6	−23.621	−23.824	−28.088	−34.112	−42.910	−66.869	0.45 128
244.5	−26.937	−27.343	−32.217	−39.188	−49.137	−77.022	0.45 196

that C_m is almost constant within the experimental error for laser power from 49.3 to 244.5 mW. Therefore, the luminescence coupling is negligible under the experimental conditions.

The photocurrent of a subcell without luminescence coupling is calculated by

$$I_i = \frac{IQE_i \cdot e \cdot P_{in} \cdot (1-g)(1-r)f(\alpha, d_1, \ldots, d_i, r_1, \ldots, r_i)}{h\nu}, \quad (5)$$

where IQE_i is the internal quantum efficiency of subcell i, e is the electron charge, P_{in} is the incident laser power, g is the shading rate of grid lines, r is the surface reflectivity of the LPC, h is the Planck constant, ν is the frequency of incident light, α is the absorption coefficient of GaAs, d_i is the thickness of subcell I, and r_i is the reflectivity at the interface between subcell i and its window layer. Function $f(\alpha, d_1, \ldots, d_i, r_1, \ldots, r_i)$ determines the light flux absorbed by subcell i. By substituting Eq. (5) into (4), C_m can be expressed by

$$C_m = \sqrt{\frac{1}{N}\sum_{i=1}^{N}\left(\frac{N \cdot IQE_i \cdot f(\alpha, d_1, \ldots, d_i, r_1, \ldots, r_i)}{\sum_{j=1}^{N} IQE_j \cdot f(\alpha, d_1, \ldots, d_i, r_1, \ldots, r_i)} - 1\right)^2}, \quad (6)$$

where N is the number of subcells. The current mismatches at different laser powers are calculated and shown in Fig. 4(a), where doping dependence of the absorption coefficient and luminescence coupling are neglected and the same interface recombination rate is used for both the upper and lower interfaces of the active layers. Figure 4(b) shows the dependence of the current mismatch degree on the absorption coefficient for our six-junction InGaAs LPC with the interface recombination rate as a parameter. It can be seen that C_m is zero when subcells are current-matched for the MJLPC designed using an appropriate absorption coefficient, and the C_m-α curve is appreciably shifted to the left only when the interface recombination rate is over 1×10^5 cm/s.

The measured C_m for the six-junction LPC is about 0.45 at 300 K, and the absorption coefficient of InGaAs can be determined based on Fig. 4(b). However, there are two possible absorption coefficients satisfying $C_m = 0.45$, i.e., around 6000 and 18 000 cm^{-1} as shown in Fig. 4(b). Due to the non-trivially different slopes of the two segments of each curve in Fig. 4(b), the actual absorption coefficient α can be confirmed by the dependence of C_m on α through varying the temperature since the absorption coefficient depends on temperature T,[27]
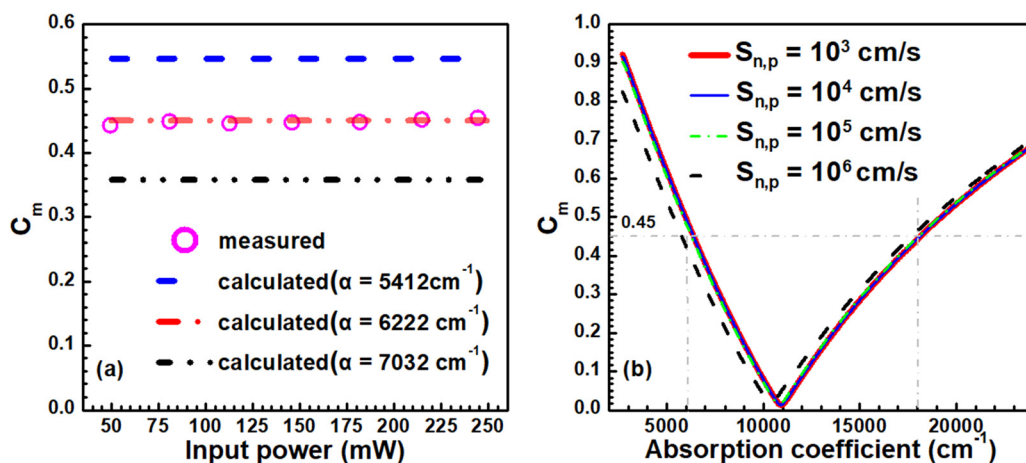

FIG. 4. (a) Calculated current mismatch degree (C_m) as a function of input laser power with an interface recombination rate of 1.5×10^4 cm/s and three absorption coefficients. (b) Calculated C_m as a function of the absorption coefficient for the six-junction InGaAs LPC using interface recombination rates ($S_{n,p}$) as a parameter.
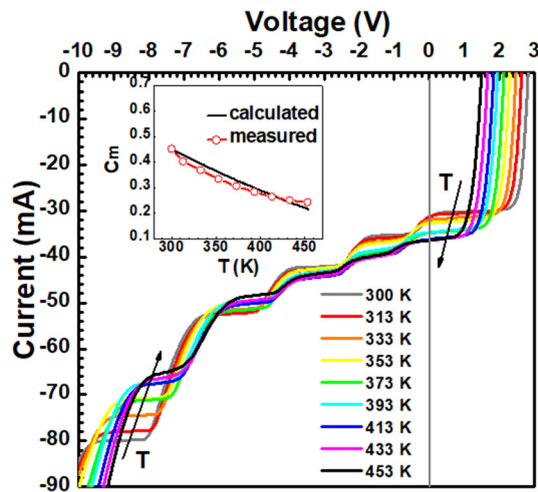
FIG. 5. Measured I–V curves of the six-junction InGaAs LPC from 300 to 453 K under a 1520 nm laser power of 0.225 W. The inset shows the measured and calculated C_m as a function of temperature.

$$\alpha = A \left[h \frac{c}{\lambda} - E_g(T) \right]^{1/2}, \qquad (7)$$

where A is a constant for a certain wavelength λ, h is the Planck constant, c is the velocity of light in vacuum, and E_g is the bandgap energy of InGaAs. The bandgap of InGaAs alloy as a function of temperature can be expressed by[28]

$$E_g(T) = E_g(0\,K) - \frac{A_1 T^2}{B_1 + T} - \left(\frac{A_2}{B_2 + T} - \frac{A_1}{B_1 + T} \right) T^2 x, \qquad (8)$$

where for $In_{1-x}Ga_xAs$ lattice matched to InP, $x = 0.47$, $E_g(0\,K) = 0.8187$ eV, $A_1 = 0.000\,419$ eV/K, $B_1 = 271$ K, $A_2 = 0.000\,58$ eV/K, and $B_2 = 300$ K. The absorption coefficient of InGaAs will increase with temperature due to the narrowing of the bandgap. Temperature-dependent I–V curves of an InGaAs MJLPC are shown in Fig. 5. It can be seen that C_m decreases with temperature, which is consistent with the left segments of the curves in Fig. 4(b). Therefore, the absorption coefficient of InGaAs is determined to be around 6000 cm^{-1} at 300 K and 1520 nm.

In sum, wide voltage range I–V characteristics of a six-junction current-mismatched InGaAs LPC are characterized and multiple steps are observed. The multiple-step I–V curve is constructed based on a series-connected-diodes model. It is shown that the steps in the curves reflect the photocurrents of the subcells in a current-mismatched MJLPC, and hence, the current mismatch degree is obtained. The absorption coefficient of InGaAs is estimated based on the relationship between the current mismatch degree and absorption coefficient in combination with the experimental temperature dependence of the current mismatch degree. This paper demonstrates an effective way to extract the subcell current mismatch and the absorption coefficient of the active layers of

an MJLPC. This has important practical implications in terms of the design of MJLPCs.

DATA AVAILABILITY

The data that support the findings of this study are available from the corresponding author upon reasonable request.

REFERENCES

[1]J. Schubert, E. Oliva, F. Dimroth, W. Guter, R. Loeckenhoff, and A. W. Bett, IEEE Trans. Electron Devices **56**, 170 (2009).
[2]S. Fafard, M. C. A. York, F. Proulx, C. E. Valdivia, M. M. Wilkins, R. Arès, V. Aimez, K. Hinzer, and D. P. Masson, Appl. Phys. Lett. **108**, 071101 (2016).
[3]S. Fafard, F. Proulx, M. C. A. York, L. S. Richard, P. O. Provost, R. Arès, V. Aimez, and D. P. Masson, Appl. Phys. Lett. **109**, 131107 (2016).
[4]Y. M. Zhao, Y. R. Sun, Y. He, S. Z. Yu, and J. R. Dong, Sci. Rep. **6**, 38044 (2016).
[5]M. C. A. York and S. Fafard, J. Phys. D: Appl. Phys. **50**, 173003 (2017).
[6]Y. R. Sun, J. R. Dong, Y. He, Y. M. Zhao, S. Z. Yu, J. P. Xue, C. Xue, J. Wang, Y. Q. Lu, and Y. W. Ding, Optoelectron. Lett. **13**, 21 (2017).
[7]J. Huang, Y. Sun, Y. Zhao, S. Yu, J. Dong, J. Xue, C. Xue, J. Wang, Y. Lu, and Y. Ding, J. Semicond. **39**, 044003 (2018).
[8]J. J. Yin, Y. R. Sun, S. Z. Yu, Y. M. Zhao, R. W. Li, and J. R. Dong, J. Semicond. **41**, 062303 (2020).
[9]C. E. Valdiviaa, M. M. Wilkins, B. Bouzazi, A. Jaouad, V. Aimez, R. Arès, D. P. Masson, S. Fafard, and K. Hinzer, in presented at Physics, Simulation, & Photonic Engineering of Photovoltaic Devices IV (2015).
[10]A. Mihaescu and P. Besnard, in presented at International Conference on Communications, Circuits, and Systems (2010).
[11]R. Finney, R. Torbeck, and N. Saedi, Laser. Surg. Med. **48**, 170 (2016).
[12]N. Gisin, G. Ribordy, W. Tittel, and H. Zbinden, Rev. Mod. Phys. **74**, 145 (2002).
[13]C. Algora and R. Pena, Artif. Organs **33**, 855 (2009).
[14]L. Wagner, S. K. Reichmuth, S. P. Philipps, E. Oliva, A. W. Bett, and H. Helmers, Prog. Photovoltaics **29**, 172 (2021).
[15]D. A. Humphreys, R. J. King, D. Jenkins, and A. J. Moseley, Electron. Lett. **21**, 1187 (1985).
[16]F. R. Bacher, J. S. Blakemore, J. T. Ebner, and J. R. Arthur, Phys. Rev. B **37**, 2551 (1988).
[17]M. S. Alam, M. S. Rahman, M. R. Islam, A. Bhuiyan, G, and A. Yamada, in International Conference on Indium Phosphide and Related Materials, Matsue, Japan, 14–18 May 2007 (IEEE, 2007), p. 343.
[18]M. Meusel, C. Baur, G. Létay, A. W. Bett, W. Warta, and E. Fernandez, Prog. Photovoltaics **11**, 499 (2003).
[19]J. García, H. Socolovsky, and J. Plá, Meas. Sci. Technol. **28**, 055203 (2017).
[20]R. R. King, D. Bhusari, A. Boca, D. Larrabee, X. Q. Liu, W. Hong, C. M. Fetzer, D. C. Law, and N. H. Karam, Prog. Photovoltaics **19**, 797 (2011).
[21]M. C. A. York, A. Mailhot, A. Boucherif, R. Arès, V. Aimez, and S. Fafard, Sol. Energy Mater. Sol. Cells **181**, 46 (2018).
[22]M. Wilkins, C. E. Valdivia, A. M. Gabr, D. Masson, S. Fafard, and K. Hinzer, J. Appl. Phys. **118**, 143102 (2015).
[23]A. W. Walker, O. Höhn, D. N. Micha, L. Wagner, H. Helmers, A. W. Bett, and F. Dimroth, in presented at Physics, Simulation, and Photonic Engineering of Photovoltaic Devices IV (2015).
[24]F. Proulx, M. C. A. York, P. O. Provost, R. Arès, V. Aimez, D. P. Masson, and S. Fafard, Phys. Status Solidi RRL **11**, 1600385 (2017).
[25]D. Xia and J. J. Krich, J. Appl. Phys. **128**, 013101 (2020).
[26]E. Lopez, O. Höhn, M. Schauerte, D. Lackner, M. Schachtner, S. K. Reichmuth, and H. Helmers, Prog. Photovoltsics **29**, 461 (2021).
[27]N. I. Iakovleva and A. V. Nikonov, J. Commun. Technol. Electron. **62**, 331 (2017).
[28]S. Paul, J. B. Roy, and P. K. Basu, J. Appl. Phys. **69**, 827 (1991).